



UPPSALA  
UNIVERSITET

UPTEC X 22005

Examensarbete 30 hp

Juni 2022

# Voxel-wise Longitudinal Analysis of Weight Gain from Different Dietary Fats using Image Registration-Based “Imiomics” Analysis

---

Vendela Andersson





## Abstract

There is an emerging global epidemic of obesity and related complications, such as type 2 diabetes (T2D). Alterations in body composition (adipose tissue, muscle volume and fat contents) are known to be associated with an increased metabolic risk. Understanding of the underlying mechanisms is key for development of novel intervention strategies. One study investigating the effect on body composition by different diets is Lipogain1. In this study, it was found that a small weight gain induced by polyunsaturated fats (PUFA, n=19) or saturated fats (SFA, n=20) had very different effects on body fat, liver fat and lean tissue mass respectively. The SFA group gained more liver fat and fat mass in general, while the PUFA group gained more muscle mass. These results were determined by magnetic resonance imaging.

The goal of this project was to visualize the results from Lipogain1 by utilizing the novel technique Imiomics. Imiomics is a method for statistical analysis of whole-body medical images. By utilizing image registration, all images are transformed to a common reference space. This enables point-wise comparisons between all images included in the analysis.

In this project, mean images of the alterations in fat content and local volume change of the two groups were created. These were used to visualize the alterations in body composition from the study. Additionally, statistical tests were used to visualize statistically significant differences between the groups.

Differences between the groups could be seen in the mean images. Mainly a higher fat content increase was seen in SFA in comparison to PUFA. There was also a larger volume expansion in fat tissue in SFA than in PUFA, while PUFA instead had a larger volume expansion in muscles. An unexpected result was also found; the liver had expanded in PUFA but not in SFA. Unfortunately, few significant differences could be visualized between the groups when the statistical test was performed.

The conclusion was that this method is promising for visualization of these kinds of studies, especially due to the potential of finding new, unexpected results. However, a somewhat larger cohort and possibly larger alterations in body composition might be needed to be able to visualize and quantify statistically significant differences between the groups on a voxel-wise level.

**Teknisk-naturvetenskapliga fakulteten**

**Uppsala universitet, Utgivningsort Uppsala**

Handledare: Joel Kullberg Ämnesgranskare: Robin Strand

Examinator: Pascal Milesi



# Populärvetenskaplig sammanfattning

Vi ser idag en växande global epidemi av övervikt och komplikationer kopplade till övervikt, som till exempel diabetes typ 2. Det är sedan tidigare känt att förändringar i kroppssammansättning, som fettvävnad och muskelvävnad, kan kopplas till en ökad risk att drabbas. Det är därför viktigt att öka förståelsen kring vad som kan orsaka sådana förändringar för att kunna utveckla nya metoder för att förhindra det. Lipogain1 är en studie som undersökte kopplingen mellan olika fetter och kroppssammansättning. I studien upptäckte man att en liten viktuppgång inducerad av fleromättade fetter (PUFA) eller mättade fetter (SFA) gav olika resultat i kroppssammansättning. SFA-gruppen fick mer leverfett och mer fettmassa överlag i jämförelse med PUFA-gruppen som istället ökade sin muskelmassa.

Resultaten från Lipogain1 bestämdes bland annat med hjälp av bilder från Magnetisk Resonanstomografi (MR). Dessa bilder har i detta projekt använts för att visualisera resultaten från Lipogain1 med en ny teknik kallad Imiomics. Imiomics är en metod för statistisk analys av medicinska helkroppsbilder. Genom att använda bildregistrering transformeras alla bilder till en gemensam referensrymd. Detta gör att varje punkt i referensbilden har en korresponderande punkt i alla bilder, och de blir då jämförbara i varje punkt, också kallad voxel. Detta kan utnyttjas till en mängd olika analyser.

I detta projekt har skillnaden i fettinnehåll mellan första och andra besöket undersökts. Ett medelvärde för denna skillnad i PUFA- och SFA-gruppen skapades i varje punkt och genom att skapa en bild från dessa kunde de gruppvisa ändringarna i fettinnehåll i olika vävnader visualiseras. Dessutom skapades medelbilder för de två grupperna för hur den lokala volymen i varje voxel hade ändrats mellan besöken. Dessa bilder användes för att försöka visualisera resultaten från Lipogain1, voxelvis fördelat över hela kroppen.

I medelbilderna sågs en viss skillnad mellan grupperna. Främst sågs en ökning i fettinnehåll i fettvävnad i SFA-gruppen i jämförelse med PUFA-gruppen. Dessutom sågs en större volymexpansion i fettvävnad i SFA-gruppen än i PUFA-gruppen, medan PUFA-gruppen istället hade en något större expansion i muskler. Dessutom hittades ett oväntat resultat; levern verkade ha ökat i volym i PUFA-gruppen, men inte i SFA-gruppen. Dessvärre kunde få statistiskt signifikanta skillnader hittas mellan grupperna när ett statistiskt test gjordes.

Slutsatsen blev att metoden är väldigt lovande för att visualisera dessa typer av studier, speciellt då det är möjligt att hitta nya och oväntade resultat. Dock skulle något större skillnader i kroppssammansättning, eventuellt i kombination med större grupper, behövas för att kunna hitta statistiskt signifikanta skillnader mellan grupperna.



# Table of contents

<b>1 INTRODUCTION</b>	<b>1</b>
1.1 Aim of project	1
<b>2 BACKGROUND</b>	<b>2</b>
2.1 Lipogain1	2
2.2 Medical Imaging	2
2.2.1 <i>Fat and Water Magnetic Resonance Imaging</i>	3
2.3 Image registration	3
2.3.1 <i>Evaluation</i>	4
2.4 Imiomics	5
2.4.1 <i>Method</i>	6
<b>3 MATERIALS AND METHODS</b>	<b>7</b>
3.1 Packages and tools	7
3.2 Data	7
3.3 Optimizing the registration pipeline	9
3.3.1 <i>Evaluation of registration pipelines</i>	10
3.4 Registrations	11
3.5 Statistical analysis	12
<b>4 RESULTS</b>	<b>13</b>
4.1 Evaluation of inter-subject registrations	13
4.2 Evaluation of intra-subject registrations	17
4.3 Statistical analysis	18
<b>5 DISCUSSION</b>	<b>23</b>
5.1 Evaluations of registrations	23
5.2 Statistical analysis	25
5.3 Limitations	26
5.4 Future work	27

<b>6 CONCLUSION</b>	<b>27</b>
<b>7 ETHICS AND CONFLICT OF INTEREST</b>	<b>28</b>
<b>8 ACKNOWLEDGMENTS</b>	<b>28</b>
<b>A APPENDIX</b>	<b>32</b>

## Abbreviations

<b>BIA</b>	Bioelectrical impedance analysis
<b>DF</b>	Deformation field
<b>DXA</b>	Dual-energy X-ray absorptiometry
<b>FF</b>	Fat fraction
<b>IQR</b>	Interquartile Range
<b>JD</b>	Jacobian Determinant
<b>MR</b>	Magnetic Resonance
<b>MRI</b>	Magnetic Resonance Imaging
<b>NCC</b>	Normalized Cross Correlations
<b>NMR</b>	Nuclear Magnetic Resonance
<b>PCC</b>	Pearson Correlation Coefficient
<b>PUFA</b>	Polyunsaturated Fatty Acids
<b>SCC</b>	Spearman Correlation Coefficient
<b>SFA</b>	Saturated Fatty Acids
<b>VME</b>	Vector Magnitude Error
<b>WF</b>	Water fraction



# 1 Introduction

There is an emerging global epidemic of obesity and related complications, such as type 2 diabetes (T2D). Alterations in body composition (adipose tissue, muscle volume and fat contents) are known to be associated with an increased metabolic risk. For example, accumulation of liver fat has been linked to the development of cardiometabolic disorders and T2D (Kotronen *et al.* 2008, 2011). Understanding of the underlying mechanisms is key for development of novel intervention strategies. One study investigating the effect on body composition by different diets is Lipogain1 (Rosqvist *et al.* 2014). In this study, it was found that a small weight gain induced by muffins baked using polyunsaturated fats (PUFA) or saturated fats (SFA) had very different effects on body fat, liver fat and lean tissue mass respectively. These results were established by magnetic resonance imaging (MRI) of all subjects before and after the weight gain.

MRI can provide anatomical and functional data such as regional tissue volume and fat/water content at millimeter scale using small 3D elements called voxels. This data can be important for studies of metabolic disorders and T2D. As the volume of data from medical imaging increases, it calls for new methods for analyzing them. Therefore, a novel technology called Imiomics has been developed (Strand *et al.* 2017) which through image registration enables a hypothesis-free analysis of whole-body medical images.

By using the Imiomics technology, the results from studies such as Lipogain1 could be visualized in a new way and used to draw further conclusions and find new, unexpected results. The image registration pipeline could be used to see differences in body composition of before and after images of the same subject, but also to visualize the differences between the SFA and PUFA groups.

## 1.1 Aim of project

The aim of this project was to try to visualize and quantify the different effects of weight gain by diets including different oils on body composition voxel-wise throughout the body. The research objectives were:

- Optimize the image registration pipeline used in Imiomics analysis for the longitudinal whole-body water-fat MR images collected in the Lipogain1 study.
- Evaluate the accuracy of the performed analysis
- Select and perform appropriate statistical methods for the analysis

## 2 Background

Below, some background for this project is presented. It starts with introducing the Lipogain1 study (Rosqvist *et al.* 2014) which this project was based on, then further giving some background information of medical imaging. Next, the concept of image registration and Imiomics is introduced.

### 2.1 Lipogain1

Intake of different dietary fats have previously been shown to have different effects on body composition. For example, a diet consisting of saturated fatty acids (SFA) have been linked to higher levels of liver fat in comparison to one consisting of polyunsaturated fats (PUFA) (Bjermo *et al.* 2012). Switching to a diet consisting of PUFA has instead been linked to a decrease in abdominal subcutaneous fat in comparison with SFA (Summers *et al.* 2002). The different effects on body composition and fat accumulation by different dietary fats was also investigated in the randomized clinical trial Lipogain1 (Rosqvist *et al.* 2014). This study was designed to let two groups of subjects ( $n=19$  and  $n=20$ ) reach a 3% weight gain induced by eating muffins baked on either PUFA or SFA. The cohort consisted of healthy males and females in the ages 20-38 years and a BMI of 18-27 kg/m<sup>2</sup>. The study found that the SFA group gained more liver fat and more fat tissue in general than the PUFA group. The PUFA group instead gained more lean tissue than the SFA group. The assessment of body composition was mainly done through whole-body MRI, but also through whole-body air displacement plethysmography (Bod Pod) and bioelectrical impedance analysis (BIA). The liver fat content was assessed using a separate, dedicated MRI scan.

### 2.2 Medical Imaging

Medical imaging is the process of reconstructing images of the body to retrieve valuable information for research, diagnostics or treatments (Meyer-Baese & Schmid 2014). It is mostly noninvasive which makes it a great tool for using clinically. Recently, there has been huge developments in this field both in the quality of the images acquired, but also in the amount of data created, which calls for an advancement in new tools for analyzing the data.

### 2.2.1 Fat and Water Magnetic Resonance Imaging

MRI is a noninvasive imaging method for visualization of the inside of the body, mainly fat and lean tissues (Meyer-Baese & Schmid 2014). Most of the signals used to create MR images comes from hydrogen atoms in fat and water molecules. The signal is derived from the nuclear magnetic resonance (NMR) which can be observed from hydrogen atoms when they are placed in an external magnetic field. From the signal, a volume image consisting of voxels can be reconstructed that shows the fat and water composition in the body. The voxels are just like pixels, but are three dimensional instead of two dimensional and each voxel gets an intensity value derived from the signal.

Due to water and fat having different resonance frequencies, a so-called chemical shift, the signals from water and fat can be separated. This can be used to reconstruct separate water and fat images of high quality (Berglund *et al.* 2010). This kind of water and fat imaging enables the possibility to measure fat and water percentage in each voxel (Berglund 2011). The fat percentage, or fat fraction (FF), can be calculated with the following formula in each voxel of the image:

$$FF = \frac{|F|}{|F| + |W|} \quad (1)$$

Where F is the fat signal and W is the water signal in that voxel. The fat fraction is quantitative, meaning that it can be compared between voxels in different images. The water fraction (WF) image can be calculated similarly.

## 2.3 Image registration

Image registration is the deformation of images to a common reference space. To do this, a transformation, or deformation field, is applied to the image which should be deformed (the moving image) which maps it to the reference space. The image can then be re-sampled with different interpolation strategies in the reference space to ensure a continuous, transformed image. The interpolation may affect the final result in for example introducing new intensities and smoothing the re-sampled image (Goshtasby 2012). Image registration mainly consists of three components, a transformation model, an objective function and an optimization method.

The transformation model can either be parametric or non-parametric (Goshtasby 2012). Examples of parametric transformation models are rigid models where the distance and the angle between points is preserved with the transformation. Another example is affine transformations where the parallelism of the image is preserved. However, in

this project, a non-parametric model developed by Ekström *et al.* have been used for the registrations (Ekström *et al.* 2018). In a non-parametric transformation model, each point of the moving image is mapped to a point in the reference space by a displacement vector specific to that point. In the method used in this project, a regularization map is used to simulate the different elasticity of the different tissues in the body, *i.e.* water and fat (Ekström *et al.* 2020). The regularization handles how similar nearby vectors in the deformation field has to be. A higher regularization leads to more similar vectors and a smoother deformation field, and vice versa. Generally, water tissue is more rigid than fat tissue and therefore usually is assigned a higher regularization.

The objective function, also known as the matching criterion, is the similarity measure that the registration seeks to optimize (Sotiras *et al.* 2013). There are many examples of matching criterions, but in this project, normalized cross-correlations (NCC), also known as Pearson’s correlation coefficient (PCC), and the sum of squared differences (SSD) has been used. Lastly, the optimization method is the method with which the matching criterion is optimized. Again, there are many methods available, but for this project a graph-cuts based approach developed by Ekström *et al.* was used (Ekström *et al.* 2018).

### 2.3.1 Evaluation

The result from image registration do typically not have one unique solution. This complicates the task of evaluation of the performance. Intuitive ways of evaluating the registration is to create mean and standard deviation images from the registrations. These are approaches for finding the image similarity, which is an important part of image registration. However, they have been shown to not be sufficient on their own (Rohlfing 2012) and should therefore be combined with other metrics to assess the performance of the registration.

Inverse consistency (Christensen & Johnson 2001) is a well known property of an image registration. If a registration is inverse consistent, it means that the transformation in one direction is the inverse of the transformation in the opposite direction. In the ideal case, where a true correspondence has been found between two images, this would be fulfilled. However, since there is no unique solution in image registration, this is seldom the case. The error in the inverse consistency can be measured by performing the registration in both directions and computing the vector magnitude error (VME) as presented in Equation 2:

$$VME = \frac{1}{|V_B|} \sum_{x \in V_B} |x - T_{B \rightarrow A} \circ T_{A \rightarrow B}(x)| \quad (2)$$

Where  $T_{B \rightarrow A}$  is the transformation from the volume  $V_B$  to the volume  $V_A$  and  $T_{A \rightarrow B}$  is the reverse transformation from  $V_A$  to  $V_B$ . The closer the VME is to 0, the closer it is to being inverse consistent and a better registration.

Another important property of a transformation is that it should be diffeomorphic. This means that both the function and the inverse should be differentiable (Sotiras *et al.* 2013). This is important since if this is not the case, it has occurred physically impossible mappings such as foldings in the registration. A great way of studying if the transform is diffeomorphic is to compute the Jacobian determinant (JD) of the deformation field at all points (Ekström 2020). If the transformation is diffeomorphic, the JD should be strictly positive at all points. A negative value of the JD indicates that physically impossible mappings have occurred, such as foldings.

The JD does not only give information about local foldings, but also about local volume change between the moving image and reference image (Leow *et al.* 2007). For example, a value of 1.1 on the JD denotes a 10% increase in local tissue volume, while a value of 0.9 denotes a 10% decrease in local tissue volume. Usually, the logarithmic transform is applied on the JD. This is due to the fact that the JD is bounded by zero below but unbounded above. This operation instead makes the JD distribution symmetric around zero. After the logarithmic transform has been applied, a negative value indicates a contraction and a positive value indicates an expansion in local tissue volume between the two images. This can be correlated to non-imaging data in a proof-of-concept evaluation. The voxel-wise correlation can be showed in a map which enables quantification and visualization of how different tissues correlate with the non-imaging metric.

## 2.4 Imiomics

Imiomics (imaging-omics) is a concept for statistical analysis of whole-body medical images (Strand *et al.* 2017). By utilizing image registration, two different images become point-wise, or voxel-wise, comparable. Each voxel in each image may contain information such as water content and fat content which can be compared between the different images by statistical analysis. The technique can be applied both to longitudinal images of the same subject, but also to group studies consisting of many subjects. In contrast to methods where only regions of interest are segmented and analyzed, Imiomics enables a holistic and hypothesis-free analysis where all of the information in the images is utilized.

### 2.4.1 Method

Assuming that the images have already been acquired, the method for performing Imiomics can be broken down into three main steps; preprocessing and reference selection, image registration, and finally a statistical analysis (Strand *et al.* 2017).

The preprocessing usually consists of creating the type of images that is going to be used for the analysis, like FF and WF images that were described in Section 2.2.1 and that were used in this project. It is also common to create some body masks for the registration pipeline. Another important step is the choice of reference space. The reference subject which all images will be deformed to is usually chosen from the cohort and the choice may influence the result significantly. Generally, it is a good idea to pick a reference subject close to the cohort mean, both in the sense of body composition and visual aspects.

The image registration is a vital step in the Imiomics analysis as it is the step that enables the point-wise correlations between the studied images. The quality of the final statistical analysis relies heavily on the quality of the registration. While reference selection can improve the result a lot, the registration might still have to do large deformations which may yield a poor registration. The registration also calls for evaluation methods to be able to conclude that the registration is satisfactory. This is not a simple task, as discussed in Section 2.3.1

Among the various types of analyzes that were initially suggested for Imiomics (Strand *et al.* 2017), three have been implemented in this project. These are correlation analysis, longitudinal analysis and group comparisons. In correlation analyzes, the correlation between the intensity value in each voxel or the local volume change in each voxel produced by the registration is correlated with a non-imaging parameter. This method have previously been shown feasible for visualization of fat and lean tissue distribution in group comparisons (Lind *et al.* 2019). In longitudinal analyzes, an individual is examined over time. In Imiomics, this is done by registration of longitudinal images followed by voxel-wise comparisons of either intensity values or local tissue volume change. Finally, in group comparison, voxel-wise comparisons are also conducted but instead between groups of subjects using statistical tests. This has previously been done to successfully visualize the relationship between metabolic syndrome and body composition (Lind *et al.* 2020).

## 3 Materials and methods

This project has mainly consisted of two parts; the registration part and the statistical analysis. The packages, tools and data that was needed for the execution, along with the methodology for the registrations and statistical analysis are presented below.

### 3.1 Packages and tools

The programming part of this project was executed in Python by utilizing various packages. All non-parametric registrations were performed by using a Python module developed by Ekström *et al.* called deform (Ekström *et al.* 2018, 2021). This is an implementation of a fast graph-cuts based non-parametric image registration method. The module has an API which utilizes SimpleITK (Lowe *et al.* 2013), an open-source multi-dimensional image analysis toolkit that was frequently used in this project for handling of images in Python. SimpleITK was used for the affine registrations in the project.

Two other libraries commonly used in this project were NumPy (Harris *et al.* 2020) and SciPy (Virtanen *et al.* 2020). NumPy has been used mainly due to its many operations applicable with multidimensional arrays. SciPy was used for the statistics performed. In addition, the software 3D Slicer (Fedorov *et al.* 2012) has been used for some visualizations in the project along with the Python library Matplotlib (Hunter 2007).

### 3.2 Data

The images used in this project was acquired in the Lipogain1 study (Rosqvist *et al.* 2014) and consisted of whole-body MRI volume images of 39 individuals. One subject was excluded from the analysis due to one of the arms being outside of the image, resulting in 38 subjects being included in the analysis. Images had been acquired from each subject before and after completion of the study. From the images, separate water and fat images had been calculated and from these, FF images and WF images had been acquired. These fraction images were used for the registrations in this project. Body masks had also been generated. Two types of masks were used in this project, one filled body mask and one mask made with spatial fuzzy c-means clustering (SFCM). The difference between these was that the SFCM mask was not filled in spaces in the body where there were no fat or water tissue, for example lungs, while the filled body mask was almost completely filled within the body. Examples of image slices are shown in Figure 1.

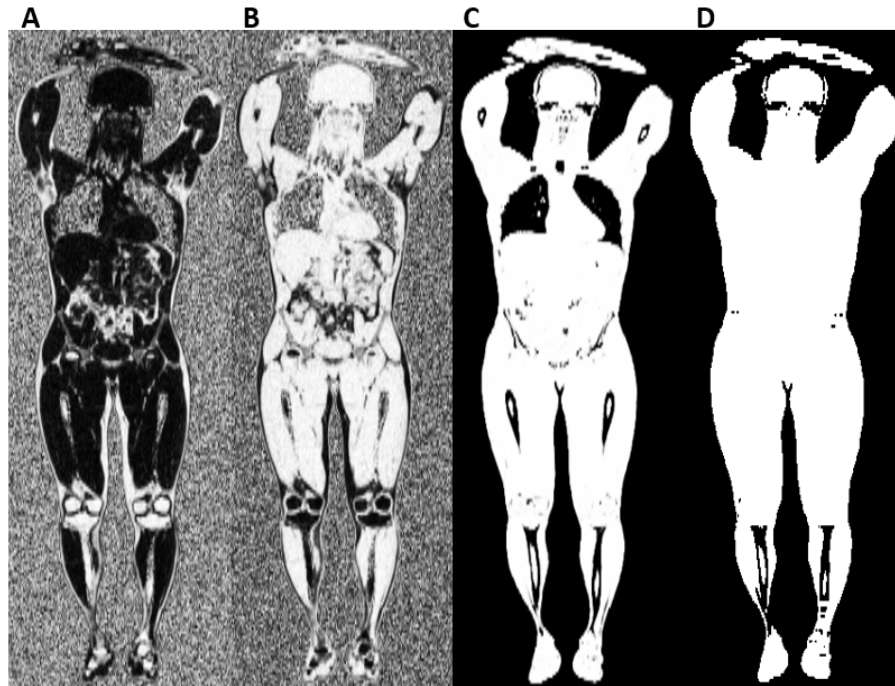


Figure 1: Examples of how a slice of the different images might look like. A is a FF image. B is a WF image. C is a SFCM body mask. D is a filled body mask.

Along with the images there were also some metadata for all the subjects which contained the group affiliation and sex of each subject, along with some calculated metrics from the study. The metrics mainly used in this project were weight, fat mass and muscle mass. All metrics were calculated for the first and second visit and from these the difference in the metrics between the first and second visit could be calculated, resulting in the delta values also used in this project. The fat mass had been calculated using Bod Pod. The muscle mass had been calculated with BIA. The results from the measurements conducted in Lipogain1 (Rosqvist *et al.* 2014) used as metadata in this project are presented in Table 1.

Table 1: Results from measurements of body weight, fat mass and muscle mass in the Lipogain1 study (Rosqvist *et al.* 2014).

Metric	PUFA 1st visit	PUFA mean change	SFA 1st visit	SFA mean change
Body Weight	67.4 +/- 8.2	1.6 +/- 0.85	63.3 +/- 6.8	1.6 +/- 0.96
Fat mass	14.4 (12.6-19.6)	0.97 +/- 1.0	12.9 (10.4-18.2)	1.5 +/- 0.70
Muscle mass	43.4 +/- 8.4	0.86 +/- 0.62	41.8 +/- 6.9	0.31 +/- 0.68

### 3.3 Optimizing the registration pipeline

The optimization of the registration pipeline mainly consisted of parameter tuning of the already existing registration method and trying different infrastructures of the pipeline on a subset of the images. Two different pipelines had to be developed for the intra-subject registrations and the inter-subject registrations.

The architectures of the pipelines are illustrated in Figure 2. The inter-subject registration pipeline starts with an affine registration of the moving filled mask to the reference filled mask to roughly align them. After that, a non-parametric registration is performed on the moving filled mask to the reference filled mask with the deformation field from the affine registration as start guess for the algorithm. This was performed to align the outer corners of the body well. Then, the backgrounds of the WF and FF images were removed with the SFCM mask and the background-filtered FF and WF images were used for the final, main registration step. This step used a dilated filled body mask to mark what areas of the images should be registered. A dilation step was added in the pre-processing to create this mask. It also utilizes a regularization map to give different regularization weights to water and fat tissue. This was also created in the pre-processing from the reference background-filtered FF and WF images. A higher regularization was used for water than for fat, since lean tissue generally is more rigid and less elastic than fat tissue.

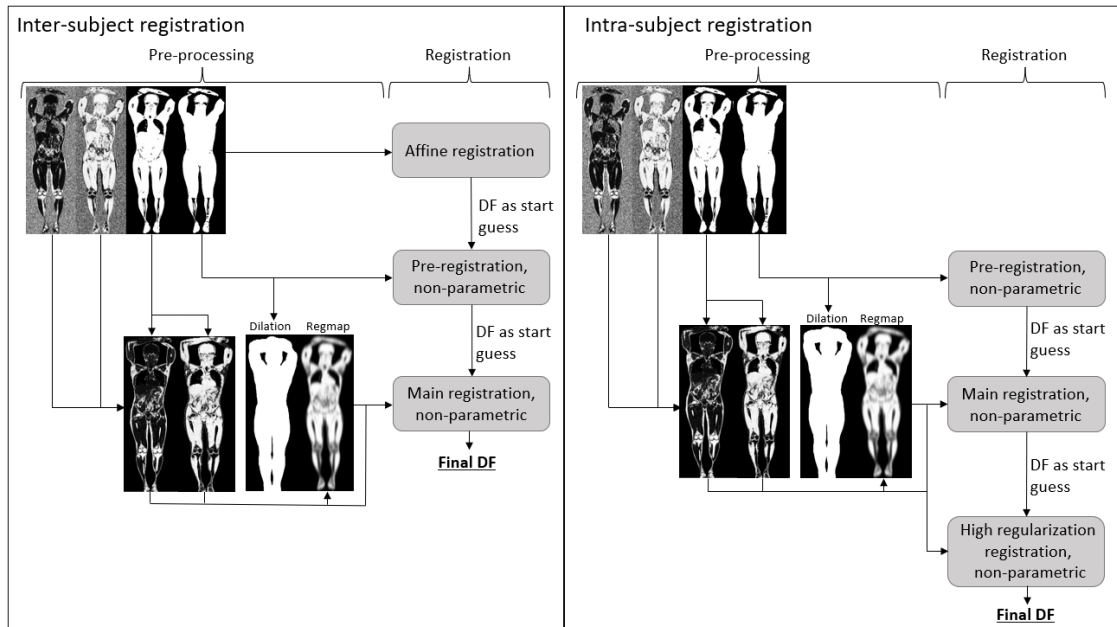


Figure 2: Schematic image of the two different registration pipelines. DF = deformation field.

The intra-subject registration pipeline starts with the pre-registration of the filled masks. It then moves on to the main registration step, which, similarly as in the inter-subject registration, uses the WF and FF images with backgrounds removed, along with dilated masks and a regularization map. The third step is a non-parametric registration step with high regularization over the whole image to smooth out the deformation field and make expansions and contractions in the registration more evenly spread out in the tissues, which was important for the statistical analysis.

Reference images were chosen for the inter-subject registrations. The reference images in this project were chosen mainly based on BMI, fat mass and visual assessment. The goal was to find references with BMI and fat mass close to the cohort mean or a bit above. Additionally, reference subjects having their feet outside of the image was chosen. One male and one female reference subject was chosen.

### **3.3.1 Evaluation of registration pipelines**

In the development of the inter-subject pipeline, it was evaluated by VME, mean maps, standard deviation maps and proof-of-concept correlation analysis to metadata. Both the mean images and standard deviation maps were used to see that the registered images were similar to each other. The mean image should ideally be as sharp as possible and different tissues should be clearly delineated as this indicates that the registered images are similar to each other. The standard deviation maps should ideally be as dark as possible since a higher intensity value indicates that the images deviates a lot from each other. The VME map should ideally also be as dark as possible since this means that the registration has a smaller VME and therefore is more inverse consistent. Light areas means a high VME and indicate that the registrations in both directions map this area to different places, that the registrations are not inverse consistent. The unit of the VME is millimeter, meaning that it shows how many millimeters the forward and backward registrations differ in their mapping of that local area.

Three types of metadata was used for the creation of correlation maps for a proof-of-concept evaluation; total body weight, muscle mass and fat mass. These metrics were correlated to the JDs to see where the metrics correlate with local volume change. For the total body weight, ideally, the correlation map should show positive correlations basically everywhere in the body since this means that if a subject has a higher body weight, it will also have a larger body. For the muscle mass, the correlation map should show positive correlations in lean tissue since this means that more lean tissue correlates with larger muscles. For the fat mass, the correlation map should show positive correlations in fat tissue since this means that higher fat mass correlate with larger fat tissue. The correlations were calculated with Spearman correlations and the color in the correlation maps indicates the value of the Spearman correlation coefficient (SCC). A

red color means a positive value of the SCC, indicating a positive correlation. Similarly, a blue color means a negative value of the SCC, thereby a negative correlation. A p-value cutoff of 0.05 was used when creating the maps, which means that pixels which are shown in color have a p-value of less than 0.05 for the correlation, and are therefore determined to be statistically significant.

The intra-subject registration pipeline was evaluated based on VME, JD maps and proof-of-concept correlation analysis to metadata. Standard deviations of the JD maps in the different groups were visually assessed. These maps show within each group were the local volume changes differ between subjects and might give a good idea of where the statistical analysis might not be as reliable. They should ideally be as dark as possible since that means a lower standard deviation. The non-image metrics used for the correlation maps of the intra-subject registration and proof-of-concept evaluation was delta weight, delta muscle mass and delta fat mass. This means that the difference between the metric for each subject at the first and second visit was used. The correlation maps are used to verify that the volume changes of tissues such as muscles and fat of each subject correlates with how much the subject gained or lost mass in those tissues. SCC was used for the correlation maps, similarly as for the inter-subject correlation maps. Similar maps are expected as for the inter-subject correlation maps, that delta weight have positive correlations with the whole body, delta muscle mass have positive correlations with muscles and delta fat has positive correlations with fat mass. However, since these metrics does not have as much variation due to all subject gaining similar amount of weight, it might be harder to find clear correlations.

### 3.4 Registrations

After the registration pipelines were finalized, the inter-subject registration of all subjects was performed both in the subject-to-reference direction, but also in the reversed direction. Then, the intra-subject registration between the before and after image of each subject was performed, also in both directions. All registrations were evaluated on previously mentioned metrics.

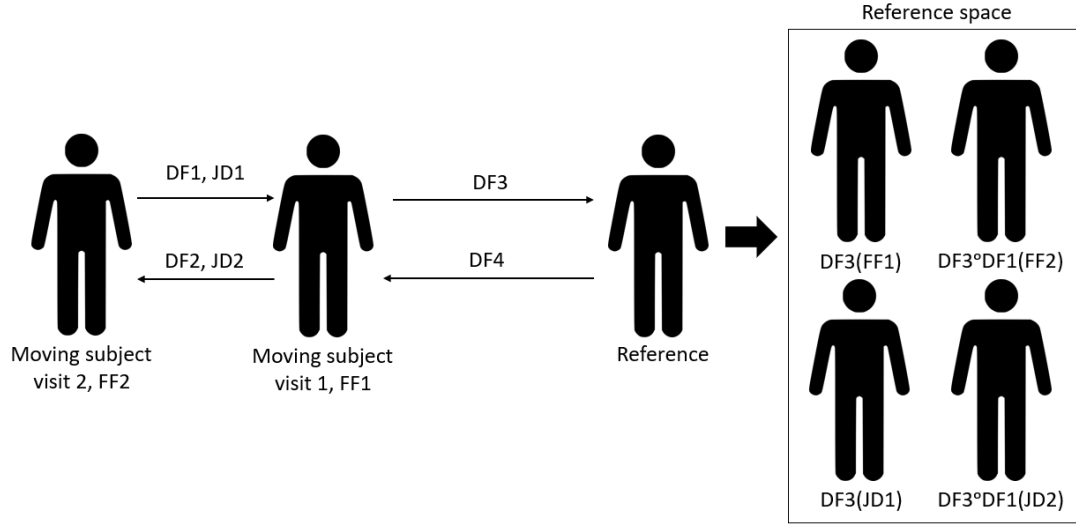


Figure 3: Schematic overview of the registrations performed. *DF* = deformation field, *JD* = Jacobian determinant map, *FF* = fat fraction image.

The images that would be used for the final statistical analysis was the FF images and the JD images. Therefore, for each subject, the intra-subject deformation field from the second visit image to the first visit image (DF1) was composed with the deformation field from the inter-subject registration between the first visit image to the reference subject (DF3). This composed deformation field was then applied to the second visit FF image (FF2) and to the JD map from the reversed intra-subject registration (JD2) to deform them to the reference space. DF3 was then applied to the first visit FF image (FF1) and to the intra-subject JD map (JD1) to deform them to reference space. A schematic overview of the registrations is illustrated in Figure 3.

### 3.5 Statistical analysis

For the visualization of the differences in body composition, the registered FF and JD images were utilized. For each subject, the first visit FF image was subtracted from the second visit FF image in the reference space, i.e. the delta fat content was calculated, to visualize where the subject had accumulated more fat. Then, separate voxel-wise mean maps for the PUFA group and the SFA group was created of all the fat difference images in each group. This was done to visualize group-wise fat accumulations. For each voxel, the corresponding intensity values from the subjects in the group were acquired and put in a vector. This intensity vector was then filtered for outliers by utilizing the interquartile range (IQR). All values outside of the span  $\pm 1.5 \cdot \text{IQR}$  from the median

was determined as outliers and excluded from further analysis. The remaining values were used to calculate the mean for that voxel. To further visualize the group differences, a voxel-wise T-test between the two groups was performed on the outlier-filtered vectors of each voxel, and images of the results were created, so-called T-maps. These maps illustrate if there are voxel-wise differences between the mean values of fat content alteration in the two groups. The maps show the value of the T-statistic when filtered for a P-value lower than 0.05. A negative T-statistic (shown with blue color in the T-maps) indicates a lower mean value, and therefore a lower increase in fat content, in the PUFA group than in the SFA group. A positive T-statistic (shown with red color in the T-maps) indicates a higher mean value in the PUFA group.

From the JD maps transformed to the reference space, separate mean maps for the PUFA and SFA group were created with the same methodology as for the fat differences to visualize where the group had changed in local body volume. Similarly as with the fat difference images, a voxel-wise T-test was performed to visualize the regions where the two groups differed. A negative T-statistic means a lower mean and a smaller volume increase in the PUFA group than in the SFA group, while a positive T-statistic means a higher mean in the PUFA group. Mean maps for the JD maps from the reversed intra-subject registration was created for the two groups to verify that the inverse results could be seen when performing the registration in the opposite direction.

## 4 Results

The results section have been divided into three parts which are presented below; evaluation of the inter-subject registrations, evaluation of the intra-subject registrations and finally the statistical analysis.

### 4.1 Evaluation of inter-subject registrations

The evaluation of the inter-subject registrations was done by visual assessment of mean images, standard deviation maps, VME maps and correlation maps between the JDs to metadata. Slices of the evaluation images are presented below. Note that these are just slices, and the evaluations was performed on the full volume images. To locate the correlations in the body in the correlation maps, the reference water image along with a partly transparent reference fat image has been added in the background.

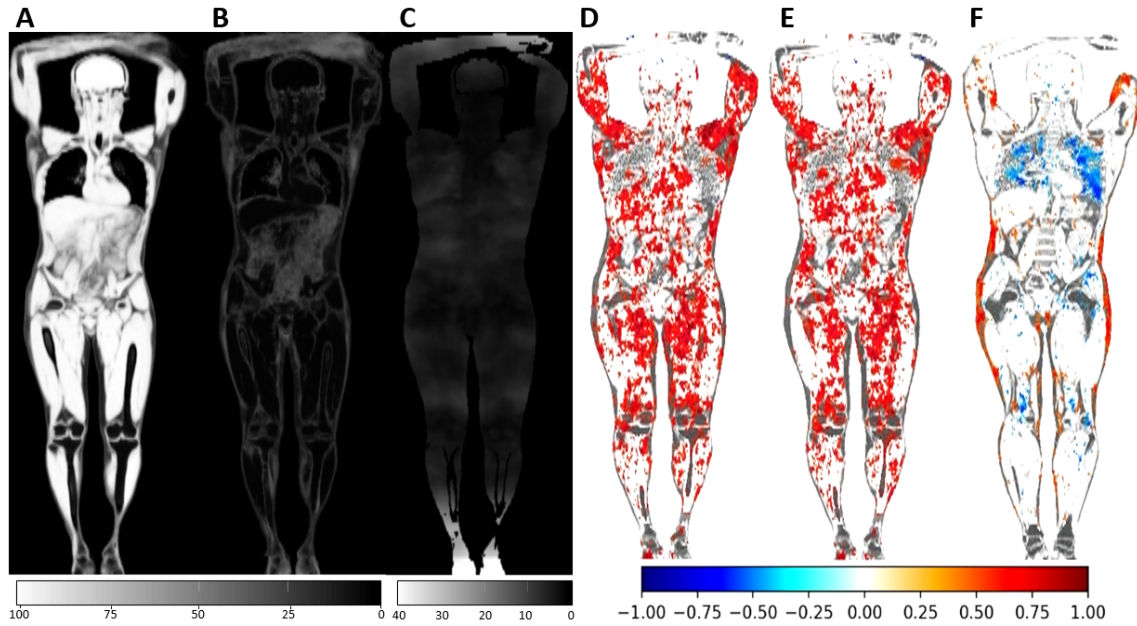


*Figure 4: Evaluations of inter-subject registrations of male subjects (n=25). A is a slice of the mean water image. B is a slice of the standard deviation map. C is a slice of the VME map. D is a slice of the correlation map of JDs to total body weight. E is a slice of the correlation map of JDs to muscle mass. F is a slice of the correlation map of JDs to fat mass. The color in the correlation maps indicates the value of the SCC. A p-value cutoff of 0.05 was used for the correlation maps.*

The evaluations for male inter-subject registration are presented in Figure 4. The mean image is relatively sharp. However, the abdomen area and underarms are quite blurry, indicating that the images look less similar here. The standard deviation map is mostly dark but lighter in the abdomen areas, underarms and feet. This means that these areas differ more in the images. The VME map is dark in most places, but lighter in feet, calves and forearms. This indicates that the registration might not be as precise in these areas.

The correlation maps for the male registration show positive correlations everywhere in the body, including weakly in fat tissue, for body weight, meaning that the whole body volume correlate with change in body weight. For the correlations to muscle mass, the whole body shows positive correlations but the subcutaneous fat does not show any clear correlations. For the correlations to fat mass, the subcutaneous fat show positive correlations but no positive correlations can be seen in muscles. It also show quite clear negative correlations with lungs, indicating that a higher level of fat mass is coupled with smaller lungs.

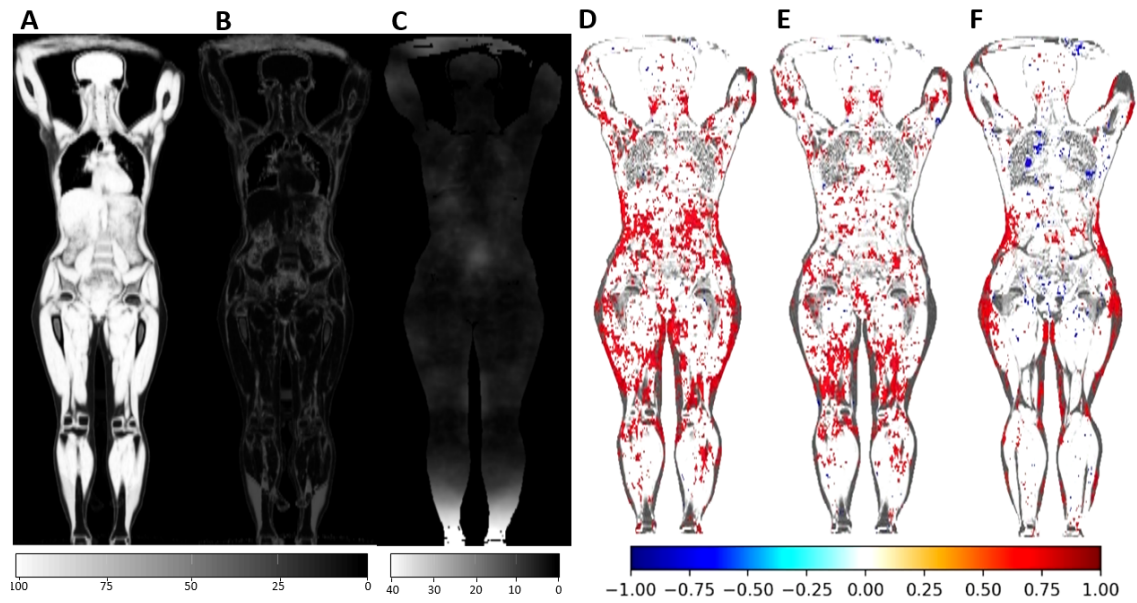


*Figure 5: Evaluations of inter-subject registrations of female subjects ( $n=11$ ). A is a slice of the mean water image. B is a slice of the standard deviation map. C is a slice of the VME map. D is a slice of the correlation map of JDs to total body weight. E is a slice of the correlation map of JDs to muscle mass. F is a slice of the correlation map of JDs to fat mass. The color in the correlation maps indicates the value of the SCC. A  $p$ -value cutoff of 0.05 has been used for the correlation maps.*

The evaluations for the female inter-subject registrations are presented in Figure 5. The mean image is quite sharp, except for the abdomen area and forearms. The standard deviation image is lighter in forearms and calves, and also a bit in abdomen. The VME image is lighter in feet, calves and forearms. These results show the same problem areas as for men; the abdomen, forearms and feet. Further results from these areas might not be as reliable.

The correlations for the female subjects are less clear than the ones for the male subjects. However, it is still possible to see positive correlations to body weight in the whole body. There are also visible positive correlations to muscle mass in the whole body, but not in the subcutaneous fat. For the correlations to fat mass, there are mainly positive correlations in subcutaneous fat tissue and not that much in muscles.

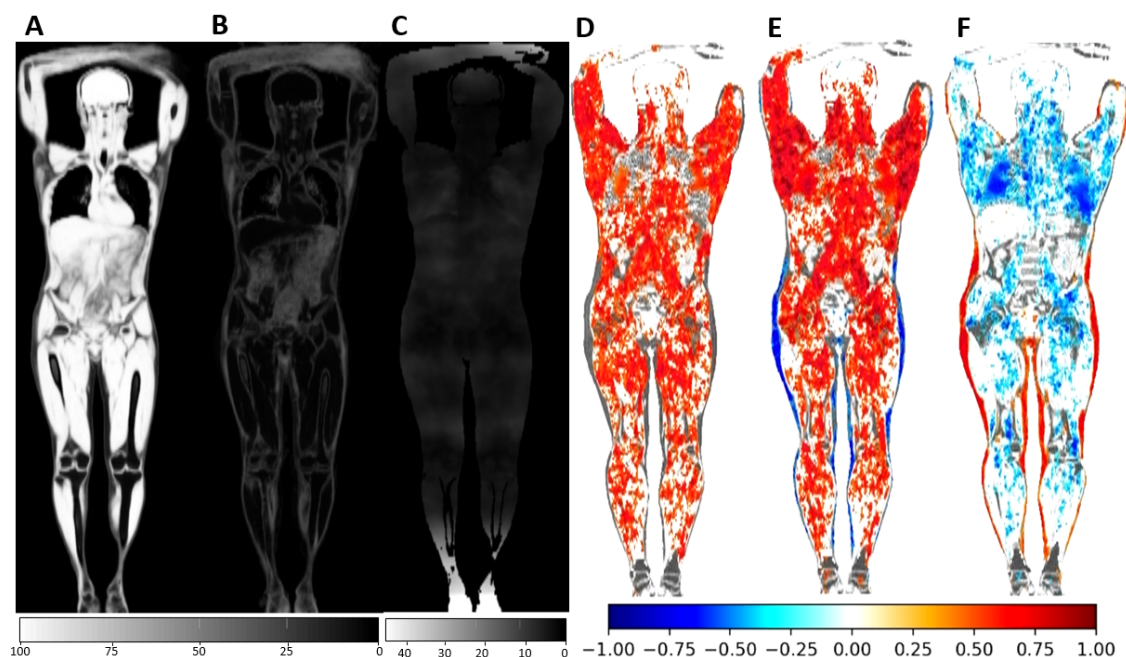


Figure 6: Evaluations of inter-subject registrations of both female and male subjects registered to a male reference ( $n=37$ ). A is a slice of the mean water image. B is a slice of the standard deviation map. C is a slice of the VME map. D is a slice of the correlation map of JDs to total body weight. E is a slice of the correlation map of JDs to muscle mass. F is a slice of the correlation map of JDs to fat mass. The color in the correlation maps indicates the value of the SCC. A  $p$ -value cutoff of 0.05 has been used for the correlation maps.

The evaluation of both females and males registered to a male reference are presented in Figure 6. The mean image still look as sharp as the one for only males, and still have issues in the abdomen and forearms. The standard deviation map is a bit brighter in the calves then the one for only males, otherwise they are similar with issues in abdomen, feet and underarms. The VME map is a bit brighter in general and especially in the calves, but otherwise it look similar.

The correlation maps for both males and females look a bit different than the ones for only males, mainly that the correlations are stronger. The whole body except the subcutaneous fat show strong positive correlations to body weight and to muscle mass. The fat tissue instead show negative correlations to muscle mass. The subcutaneous fat show strong positive correlations to fat mass while the rest of the body and especially lungs shows negative correlations. The expected correlations seem to be amplified when including females in the registration to a male reference.

*Table 2: Mean VME and mean number of negative JDs (NJD) for males and females separately, for both together to the same male reference and for the intra-subject registration.*

<b>Metric</b>	<b>Male</b>	<b>Female</b>	<b>Both</b>	<b>Intra-subject</b>
<b>Mean VME (mm)</b>	5.14	5.28	5.43	1.95
<b>Mean NJDs</b>	3.16	4.91	3.14	0.00

Further, the mean VME of the three groups and the mean number of negative JDs (NJDs) were used to verify that it is appropriate to include females in the registration to a male reference. These results are presented in Table 2. The mean VME is slightly higher when registering females and males to the same male reference than when registering them separately. The mean number of NJDs was not higher.

## 4.2 Evaluation of intra-subject registrations

The evaluation of the intra-subject registrations was done by observing a mean VME image, a standard deviation image of all JD maps produced in the two groups and by proof-of-concept correlation analysis. To locate the correlations in the body in the correlation maps, the reference water image along with a partly transparent reference fat image has been added in the background.

The standard deviation maps in Figure 7 gives an idea of where the volume changes in each group differs. The maps from both groups seem to have differences in the same places. It can be seen that the arms, head, lungs and calves have higher differences, along with the top of the liver and some parts of the abdomen. There are also some lighter areas in the outer side of the thighs. The VME map shows errors in arms, head and calves. It also show some errors in thighs. However, as presented in Table 2, the mean VME for all intra-subject registrations together is lower than the mean VME for the inter-subject registration, indicating a good registration. The mean number of negative JDs was 0 which indicates that no foldings have taken place in the registration. Due to all evaluations, both from the inter- and intra-subject registrations, pointing towards uncertain registrations in arms and lower calves and feet, results from these areas will not be taken into consideration in the statistical analysis.

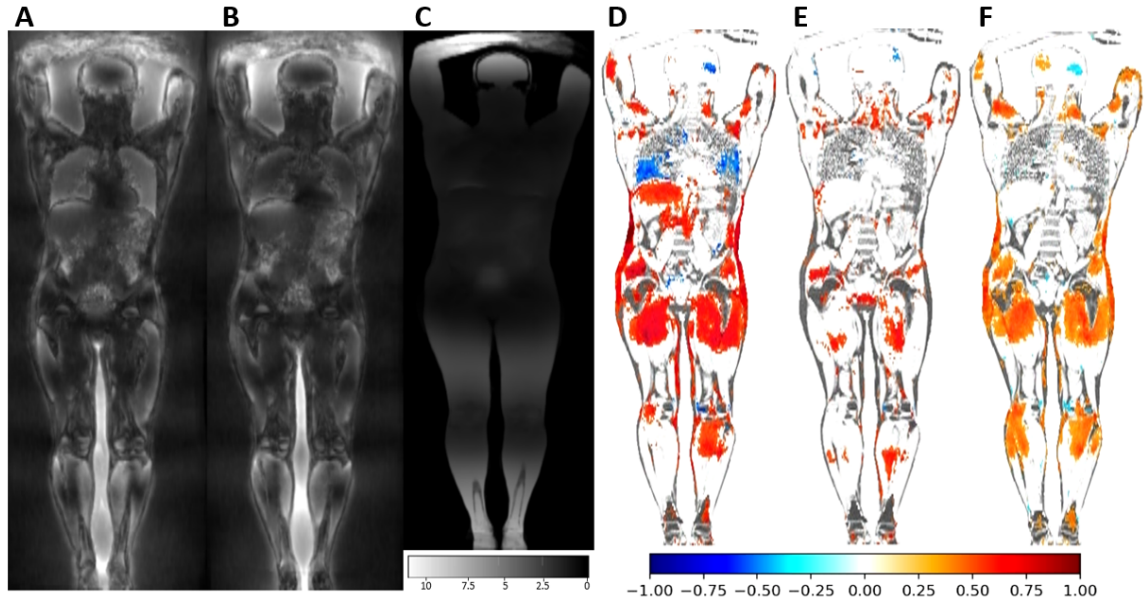


Figure 7: Evaluations of intra-subject registrations. A is a slice of the voxel-wise standard deviation map of all JD maps produced from the PUFA group deformed to a common, male reference space ( $n=18$ ). B is a slice of the voxel-wise standard deviation map of all JD maps produced from the SFA group deformed to a common, male reference space ( $n=20$ ). C is a slice of the mean VME map of all intra-subject registrations ( $n=38$ ). D is a slice of the correlation map between all intra-subject registration JD maps and delta body weight ( $n=38$ ). E is a slice of the correlation map between all intra-subject registration JD maps and delta muscle mass. F is a slice of the correlation map between all intra-subject registration JD maps and delta fat mass. The color in the correlation maps indicates the value of the SCC. A  $p$ -value cutoff of 0.05 has been used for the correlation maps.

The correlation maps shows strong positive correlations between weight and the local volume change in thighs and subcutaneous fat. Some positive correlations in thighs can also be seen for muscle mass. For fat mass, both subcutaneous fat and muscles in thighs positively correlates.

### 4.3 Statistical analysis

The statistical analysis consisted of trying to visualize the results from the Lipogain1 study (Rosqvist *et al.* 2014). This was done by creating mean maps of the JD maps and fat difference maps for the intra-subject registrations in the two groups, when registered to the common reference space. Voxel-wise T-tests for the fat differences and JD maps

were performed between the PUFA and SFA groups to visualize the differences between the groups. Slices of these results are presented below.

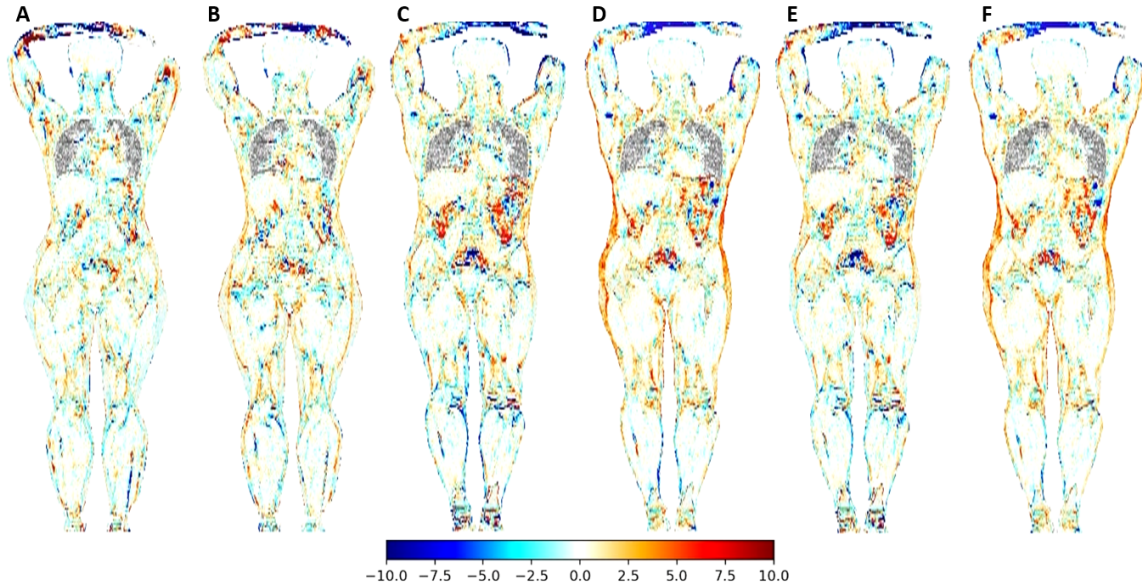


*Figure 8: Mean difference in fat content between first and second visit. Red color indicates higher fat content in the second visit than in the first visit, blue color indicates lower fat content in the second visit than in the first visit. A is female subjects in the PUFA group (n=6). B is female subjects in the SFA group (n=6). C is male subjects in the PUFA group (n=12). D is male subjects in the SFA group (n=14). E is both female and male subjects in the PUFA group (n=18). F is both female and male subjects in the SFA group (n=20).*

The mean differences in fat content between the first and second visit in the different groups are presented in Figure 8. For females, a weak increase in fat content can be seen along the borders between muscles and subcutaneous fat in both the PUFA and SFA group, however a bit clearer in the SFA group. Tendencies of more visceral fat in the abdomen for SFA is also visible. For males in the SFA group, a clear increase in fat content can be seen in the subcutaneous fat. This pattern is not as clearly observable in the PUFA group. There also seem to be some increase in fat content in the visceral fat in the abdomen in the SFA group in comparison with the PUFA group. A similar pattern with the subcutaneous and visceral fat can be observed when both males and females are bundled together in the same groups.

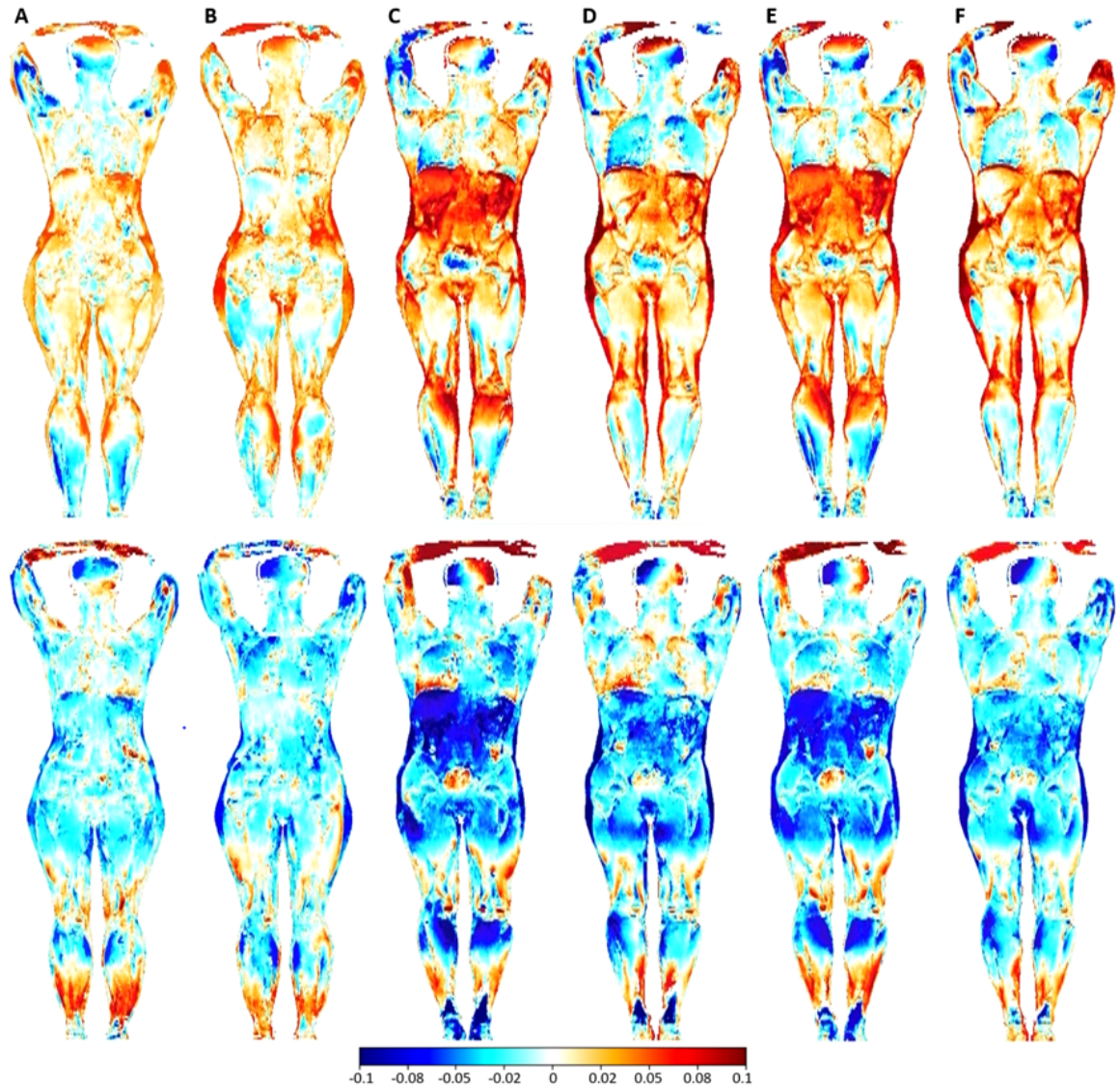


Figure 9: Mean JD maps from the intra-subject registrations. The top row is the forward registration, meaning the registration of the second visit to the first visit. Red color indicate a positive value of the JD, hence a larger local volume in the second visit in comparison to the first visit. A blue color indicates a negative value of the JD, hence a smaller local volume in the second visit in comparison to the first visit. The second row show the reversed registration, hence the registration of the first visit to the second. A red color indicate a smaller volume in the second visit and a blue color indicate a larger local volume in the second visit. The forward registration of a group is placed above the reversed registration of the same group for easier comparison. A is female subjects in the PUFA group ( $n=6$ ). B is female subjects in the SFA group ( $n=6$ ). C is male subjects in the PUFA group ( $n=12$ ). D is male subjects in the SFA group ( $n=14$ ). E is both female and male subjects in the PUFA group ( $n=18$ ). F is both female and male subjects in the SFA group ( $n=20$ ).

The mean JD maps showing the voxel-wise mean JD, and therefore the mean local volume change between the first and second visit, of the different groups are presented in Figure 9. For females, larger volumes in the second visit can be seen in subcutaneous fat tissue and also some in the abdomen. The expansions seem to be larger in the SFA group than the PUFA group, indicated by a darker red color. The PUFA group shows larger volumes for the second visit in the muscle mass in thighs, in contrast to the SFA group which show smaller volumes here. Males show similar patterns for subcutaneous fat. However, there seem to be more expansions in the abdomen in PUFA in comparison with SFA, especially in the liver and various other organs. Both groups seem to experience expansions in thighs. When both males and females are analyzed together, the pattern in the subcutaneous fat remains. There also seem to be more expansions in the muscles in thighs in PUFA in comparison with SFA. The expansions in abdomen in the PUFA group also remains.

The mean JD maps from the reversed intra-subject registration is also shown in Figure 9. The maps generally looks like the inverse of the JD maps in the forward direction. Areas which are shown in bright red in the forward are shown in blue in the reversed direction. This shows that the same results are obtained when performing the registration in the opposite direction, and that the registration is stable in both directions.

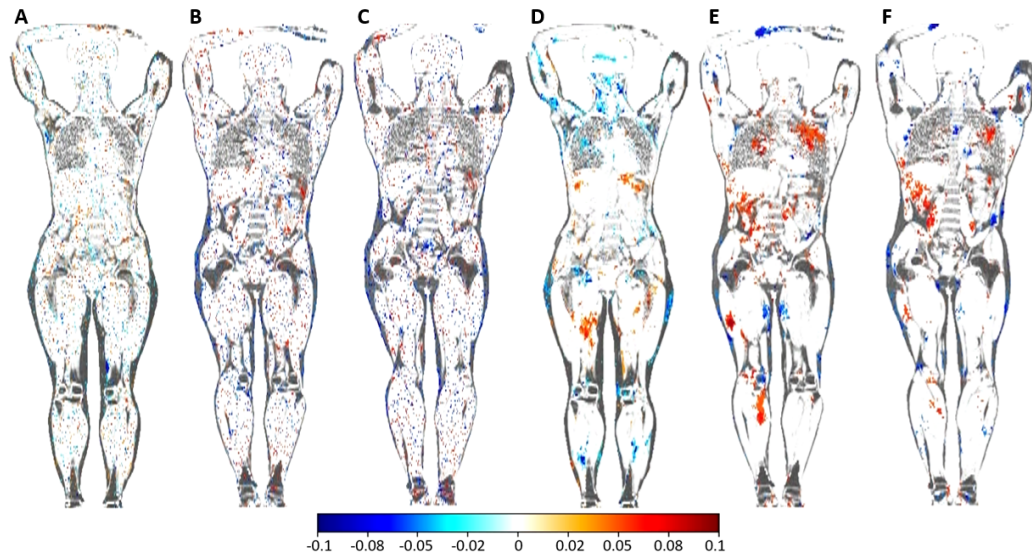


Figure 10: Voxel-wise T-tests between the PUFA and SFA group for the difference in fat content and JD maps. Red color indicates a positive T-statistic, thus a larger mean value in the PUFA group than the SFA group. A blue color indicates a negative T-statistic, thus a smaller mean value in the PUFA group than in the SFA group. All maps have a P-value cutoff of 0.05. A is the T-test between the difference in fat content of the female PUFA (n=6) and SFA (n=6) group. B is the T-test between the difference in fat content of the male PUFA (n=12) and SFA (n=14) group. C is the T-test between the difference in fat content of the PUFA (n=18) and SFA (n=20) group consisting of both females and males. D is the T-test between the JD maps of the female PUFA (n=6) and SFA (n=6) group. E is the T-test between the JD maps of the male PUFA (n=12) and SFA (n=14) group. F is the T-test between the JD maps of the PUFA (n=18) and SFA (n=20) group consisting of both females and males.

The voxel-wise T-tests for the fat content difference and JD maps are presented in Figure 10. The T-test of the difference in fat content between PUFA and SFA in females show no clear patterns. For males, a weak negative pattern is visible in subcutaneous fat, indicating less fat content increase in PUFA than in SFA. This pattern is also visible in the map including both females and males. The T-test for the JD maps show a weak negative pattern in subcutaneous fat around the hip region for females. This pattern is not as visible in males, but when including both females and males it is weakly visible again. This indicates that the PUFA group gained less subcutaneous fat than the SFA group. A weak positive pattern can be seen in some spots muscles in thighs for the three maps which indicates a larger increase of muscle mass in the PUFA group than in the SFA group. However, there are also some spots with negative patterns. There are also quite clear positive pattern in abdomen, specifically around the liver, indicating that the PUFA group has expanded more here than the SFA group. Overall, most patterns in the t-maps have P-values above 0.05 and are therefore not considered statistically significant.

## 5 Discussion

The goal of this project was to visualize and quantify the different effects on body composition of weight gain by diets including different oils by utilizing Imiomics. This was done by performing image registration, evaluating the registrations, and perform various statistical tests. This is not a simple task, both since it was a quite small data set and also small changes distributed over a large number of voxels.

### 5.1 Evaluations of registrations

Two of the aims of this project was to optimize a registration pipeline for the Lipogain1 MR images along with evaluating the pipeline. The results of the evaluations were presented in Section 4.1 and 4.2. All of the inter-subject registration evaluations points at lower registration accuracy in mainly arms, feet and abdomen. This could be explained by these areas being the parts of the body which vary the most between subjects in the images. The arm positioning was not always standardized in the images. Some subjects had the right arm under the left and some had the other way around. This makes it impossible for the algorithm to correctly register the arms without introducing foldings in the registrations, which is generally minimized. Some subject also had their arms in direct connection with the head, leading to curious deformations in both arms and head. The feet also experience problems with positioning, some people having them close together, other having them far apart. Another problem with the images was that some subjects had their feet outside of the image while some had them inside. Reference subjects were chosen that had their feet outside of the image. This was chosen since it was a less advanced problem for the registration pipeline to register subjects with their feet inside of the image to a reference with its feet outside, than in the reversed case. This led to that the registration to the reference generally performed well. However, in the opposite direction, the reference image will be registered to multiple subjects having their feet inside of the image. This is a difficult problem and leads to a high variability in the registration and is one of the reasons why the VME is so high in feet. This means that the error is mainly in the backward direction and not in the forward direction, the later being the one used for further studies in the project.

The correlation maps generally showed what was expected for all tests. The correlation maps for weight had positive correlations everywhere in the body, the correlation maps for muscle mass had positive correlations almost everywhere except for fat tissue and the correlation maps for fat mass had positive correlations to fat tissue. This verify that the registration pipeline performed well. However, the correlation maps for the female

subjects were less clear than the other correlation maps. This was probably due to there being so few female subjects ( $n=11$ ) that was deformed. The correlation maps for both male and female subjects instead show very strong correlations. This is probably due to when adding the females to the males, more variability is added to the cohort, enabling stronger correlations. The female subjects generally had more fat mass and less muscle mass than the male subjects. This leads to the negative correlations in fat mass when correlating to muscle mass; when a subject has less muscle mass (typically a female) it generally has more fat mass in comparison to the cohort, due to females generally having more fat mass and less muscle mass. Since the correlation maps actually got clearer when including the females in the registration to a male reference, this suggests that including females could be a good idea for further analysis since the registration does not become that much worse and it would increase the number of subjects in each group which could improve the statistical power of the statistical analysis. Therefore, for further analysis the females and males were bundled together into one PUFA group and one SFA group, as well as being analyzed separately.

The intra-subject registration is a bit harder to evaluate due to the subjects not being registered to a common reference. The logic for verifying the intra-subject registration was that if the inter-subject registration works, then the intra-subject registration should perform at least as well since it is a less advanced problem. In the standard deviation maps of the JD maps it can be seen that the volume changes seem to differ a lot in arms and calves, which also can be seen in the VME map. This is most likely because of the same reason as for the inter-subject registration; high variability in the positioning of arms and legs in the images. However, the VME map is darker than that for inter-subject registration, indicating that the intra-subject registration performs better. Additionally, the mean VME is lower and there are no NJDs.

The correlation maps for the intra-subject registration weakly shows what was expected, but do not show as clear correlations as the inter-subject registrations. This could be explained by these showing the correlation to the delta metrics, which has a lot less variation since all subjects have gained a similar amount of weight. This complicates the task of finding correlations. There is also larger errors in the delta values than in the individual values. Since two values are subtracted, both their individual errors are included in the delta value and the final error could be as much as duplicated. This could make it more complicated to find any correlations since the correlations might be weak even without the errors. In the delta fat mass correlation map, correlations can be seen not only in fat tissue, but also in muscles in thighs. This is probably due to the fact that most subjects that gained weight increased both their fat and lean tissue mass, leading to both correlating with each other.

## 5.2 Statistical analysis

As previously mentioned, an aim of the project was to perform statistical analysis to visualize the results of the study. For this, mean maps of the alterations in fat content and JD maps were created and T-tests were made to visualize the differences between the groups. The maps of mean difference in fat content show that the SFA group seem to gain more subcutaneous fat. This is in line with the explicit measures from the Lipogain1 study (Rosqvist *et al.* 2014) which found a higher gain of subcutaneous fat and fat tissue in general for the SFA group in comparison to PUFA. However, no visible fat gain can be seen in liver in the SFA group, even though this was found in Lipogain1 (Rosqvist *et al.* 2014). In the study, this gain was measured with a dedicated MRI scan of the liver, not with the whole-body MRI images used in this project. The reason why it is not visible in the whole-body images could be that they are simply of too low resolution and that the fat content, even after the increase, is so low that it is not detectable with this analysis.

The JD mean maps show larger volume in subcutaneous fat in the second visit than in the first visit for both groups. However, the expansion seem to be larger for the SFA group. This is in line with the Lipogain1 study (Rosqvist *et al.* 2014) and with previous studies showing that a PUFA diet leads to less subcutaneous fat in comparison with a SFA diet. In the maps for females and for the mixed maps it is also possible to see a slight volume increase in muscles in thighs in the PUFA group in comparison to the SFA group. This is in line with Lipogain1 (Rosqvist *et al.* 2014) since it was found that the PUFA group gained more muscle mass. This difference is however not as clear in only males, and it is generally very weak in the other maps too. This difference might be hard to detect since it was only about a 2% increase of the lean tissue mass in PUFA (Rosqvist *et al.* 2014) and it is over a quite large volume, hence, many voxels. The fat volume increase is easier to visualize since it was a quite large increase (over 10% in SFA (Rosqvist *et al.* 2014)) and over a relatively small volume, making it more concentrated. The reversed JD maps show the same results as the forward mean maps, which verifies the results.

There were some interesting results around the liver in the mean JD maps. All maps show a bright red line at the top of the liver. This effect most likely comes from the so-called "water-fat-swap artefact". This is an artefact from the construction of the water and fat images where sometimes, the top of the liver is confused to be fat instead of water. This leads to a sharp edge at the top of the liver which in turn leads to peculiar registration effects which might be visible in the JD maps. Another interesting finding was that the volume of the liver seemed to increase to the second visit in the PUFA group, but not as much in the SFA group. There is no clear explanation of this finding and more research in the area is needed to investigate this.

The T-tests shows the voxel-wise significant differences between the PUFA and SFA group. Unfortunately, it seems as though most differences are not significant ( $P > 0.05$ ). In the T-tests of the fat contents, a blue pattern in the subcutaneous fat would ideally be seen as this would mean a significantly lower mean for the PUFA group than the SFA group. This pattern is weakly visible. For the T-tests of the JD maps, ideally a red pattern in lean tissue and a blue pattern in fat tissue would be seen. Some spots indicating such patterns can be seen in some places, but they are not very reassuring. The main reason for this might be that the differences are quite small, as they should be, and that there are few subjects in each group which lowers the statistical power of the analysis. T-tests without any P-value cutoff can be found in Appendix I. Here, the expected patterns can be seen quite clearly, but unfortunately, most were found non-significant.

### 5.3 Limitations

The goal of this project was to quantify and visualize the body composition differences between the two groups. This has been achieved by comparing voxels as if they were independent units of information. However, since the voxels are parts of tissues and we are actually interested in the changes in the whole tissues, the voxels are not independent from each other. This is a limitation since there might be stronger patterns in for example the T-tests or the JD maps if the dependence between the voxels was accounted for. A tissue specific smoothing function was developed to try to mimic this by lowering the resolution within the tissues, thereby receiving a more global result. However, the results from this did not improve the T-tests.

Additionally, it was not investigated in Lipogain1 (Rosqvist *et al.* 2014) exactly where in the body the subjects actually gained the weight, only that the fat and lean tissue mass was increased. It is possible that the subjects gained weight in different regions of the body due to different lifestyles, sex and genetics. This would further complicate the visualization since there would be large divergences within the groups and less coherent patterns.

Another limitation of this type of study is that the interpolation of the images when they are registered might introduce new values in the image. This mean that data might be created or lost and there is a risk that the analysis does not become as precise. This was minimized by deforming all images to the reference space and performing all analyzes there, since all images then would experience similar interpolation artefacts. However, the artefacts will still be there.

Image registration does not have one single, true solution. This means that there is almost

always errors in the registration, and another solution could be equally true. The choice of reference image can also influence the outcome significantly. Problems can arise if the body position of the reference subject is deviating in some way, for example if the feet are placed too close together or if the arms are positioned in a different way than in the other images. There may also be issues if it has a deviating body composition, such as abnormal levels of fat or muscle mass in comparison to the cohort. If a too small reference subject is chosen, there is a risk of losing data since most of the moving subjects will have to be contracted when registered. On the other hand, if a too large reference subject is chosen, there might be issues with many large expansions and the registration interpolation creating data that actually does not exist.

Generally, the results of this project most likely would have improved if there were more subjects in the group, larger changes in body composition and larger differences between the groups.

## 5.4 Future work

This project found an unexpected result of an enlarged liver in the PUFA group. This was not investigated in the Lipogain1 study (Rosqvist *et al.* 2014), and it would be of value to actually segment the liver in all subjects and analyze the size. If it actually got larger in the PUFA group, that would validate the results from this study as well as enabling new insights in how different dietary fats might influence the liver.

This project shows potential for this type of analysis for similar studies in the future. Even the small changes in body composition that was studied in this project was somewhat visible, and with larger changes this could work well.

## 6 Conclusion

In conclusion, it was to some extent possible to visualize the results from the Lipogain1 study over the whole body region. However, to get sufficiently satisfying results, more subjects and/or a higher weight gain would probably be a good idea. Still, the results are promising and shows that Imiomics could be suiting for similar studies. Additionally, if the size of the liver was actually investigated and found to increase in size in PUFA, it would not only give insights in the effect of dietary fats on the liver, but also further verify the Imiomics method as a hypothesis-free analysis to find new, unexpected results.

## 7 Ethics and conflict of interest

All subjects included in the Lipogain1 study (Rosqvist *et al.* 2014) gave their written informed consent prior to participating in the study and ethical approval had been received for the study and for analysis of the MR images acquired.

When working with human subjects it is always important to consider the ethics of the project. It was previously known that a diet consisting of SFA had been linked with higher levels of liver fat, which in turn has been connected to metabolic disorders. Therefore, the ethics of conducting a study where subjects gain weight by SFA could be questioned. However, at the small levels of weight gain that was reached in the Lipogain1 study (Rosqvist *et al.* 2014), there should be no risk for the subjects, especially since they were all healthy individuals.

## 8 Acknowledgments

First of all I would like to thank my supervisor Joel Kullberg for giving me the opportunity to do this project, for all the support and endless amount of ideas during the work. I would also like to thank the PET/MR research group for a welcoming and inspiring work environment and for all the support with, and interest in my project. Next, I want to thank my subject reader Robin Strand for all feedback, inputs and ideas to the project. Lastly, I would like to thank my examiner Pascal Milesi and to the course coordinator Lena Henriksson for help and support during the course.

## References

- Berglund J. 2011. Separation of Water and Fat Signal in Magnetic Resonance Imaging : Advances in Methods Based on Chemical Shift. Publisher: Acta Universitatis Upsaliensis.
- Berglund J, Johansson L, Ahlström H, Kullberg J. 2010. Three-point dixon method enables whole-body water and fat imaging of obese subjects. *Magnetic Resonance in Medicine* 63: 1659–1668. \_eprint: <https://onlinelibrary.wiley.com/doi/pdf/10.1002/mrm.22385>.
- Bjermo H, Iggman D, Kullberg J, Dahlman I, Johansson L, Persson L, Berglund J, Pulkki K, Basu S, Uusitupa M, Rudling M, Arner P, Cederholm T, Ahlström H, Risérus U. 2012. Effects of n-6 PUFAs compared with SFAs on liver fat, lipoproteins, and inflammation in abdominal obesity: a randomized controlled trial. *The American Journal of Clinical Nutrition* 95: 1003–1012.
- Christensen G, Johnson H. 2001. Consistent image registration. *IEEE Transactions on Medical Imaging* 20: 568–582. Conference Name: IEEE Transactions on Medical Imaging.
- Ekström S. 2020. Efficient GPU-based Image Registration : for Detailed Large-Scale Whole-body Analysis Publisher: Acta Universitatis Upsaliensis.
- Ekström S, Kullberg J, Ahlström H, Strand R, Malmberg F. 2020. Deformable Image Registration of Volumetric Whole-body MRI: An Evaluation.
- Ekström S, Malmberg F, Ahlström H, Kullberg J, Strand R. 2018. Fast Graph-Cut Based Optimization for Practical Dense Deformable Registration of Volume Images. *arXiv:1810.08427 [cs]* ArXiv: 1810.08427.
- Ekström S, Pilia M, Kullberg J, Ahlström H, Strand R, Malmberg F. 2021. Faster dense deformable image registration by utilizing both CPU and GPU. *Journal of Medical Imaging* 8: 014002.
- Fedorov A, Beichel R, Kalpathy-Cramer J, Finet J, Fillion-Robin JC, Pujol S, Bauer C, Jennings D, Fennessy F, Sonka M, Buatti J, Aylward S, Miller JV, Pieper S, Kikinis R. 2012. 3D Slicer as an Image Computing Platform for the Quantitative Imaging Network. *Magnetic resonance imaging* 30: 1323–1341.
- Goshtasby A. 2012. Image Registration - Principles, Tools and Methods. *Advances in Computer Vision and Pattern Recognition*. Springer London Ltd.

- Harris CR, Millman KJ, van der Walt SJ, Gommers R, Virtanen P, Cournapeau D, Wieser E, Taylor J, Berg S, Smith NJ, Kern R, Picus M, Hoyer S, van Kerkwijk MH, Brett M, Haldane A, del Río JF, Wiebe M, Peterson P, Gérard-Marchant P, Sheppard K, Reddy T, Weckesser W, Abbasi H, Gohlke C, Oliphant TE. 2020. Array programming with NumPy. *Nature* 585: 357–362. Number: 7825 Publisher: Nature Publishing Group.
- Hunter JD. 2007. Matplotlib: A 2d graphics environment. *Computing in Science & Engineering* 9: 90–95.
- Kotronen A, Juurinen L, Hakkarainen A, Westerbacka J, Cornér A, Bergholm R, Yki-Järvinen H. 2008. Liver Fat Is Increased in Type 2 Diabetic Patients and Underestimated by Serum Alanine Aminotransferase Compared With Equally Obese Nondiabetic Subjects. *Diabetes Care* 31: 165–169.
- Kotronen A, Yki-Järvinen H, Sevastianova K, Bergholm R, Hakkarainen A, Pietiläinen KH, Juurinen L, Lundbom N, Sørensen TI. 2011. Comparison of the Relative Contributions of Intra-Abdominal and Liver Fat to Components of the Metabolic Syndrome. *Obesity* 19: 23–28. [\\_eprint: https://onlinelibrary.wiley.com/doi/pdf/10.1038/oby.2010.137](https://onlinelibrary.wiley.com/doi/pdf/10.1038/oby.2010.137).
- Leow AD, Yanovsky I, Chiang MC, Lee AD, Klunder AD, Lu A, Becker JT, Davis SW, Toga AW, Thompson PM. 2007. Statistical Properties of Jacobian Maps and the Realization of Unbiased Large-Deformation Nonlinear Image Registration. *IEEE Transactions on Medical Imaging* 26: 822–832.
- Lind L, Kullberg J, Ahlström H, Michaëlsson K, Strand R. 2019. Proof of principle study of a detailed whole-body image analysis technique, “Imiomics”, regarding adipose and lean tissue distribution. *Scientific Reports* 9: 7388. Number: 1 Publisher: Nature Publishing Group.
- Lind L, Strand R, Michaëlsson K, Ahlström H, Kullberg J. 2020. Voxel-wise Study of Cohort Associations in Whole-Body MRI: Application in Metabolic Syndrome and Its Components. *Radiology* 294: 559–567. Publisher: Radiological Society of North America.
- Loweckamp BC, Chen DT, Ibáñez L, Blezek D. 2013. The Design of SimpleITK. *Frontiers in Neuroinformatics* 7: 45.
- Meyer-Baese A, Schmid V. 2014. Pattern Recognition and Signal Analysis in Medical Imaging. *Pattern Recognition and Signal Analysis in Medical Imaging (Second Edition)*, Academic Press, Oxford, i.

- Rohlfing T. 2012. Image Similarity and Tissue Overlaps as Surrogates for Image Registration Accuracy: Widely Used but Unreliable. *IEEE transactions on medical imaging* 31: 153–163.
- Rosqvist F, Iggman D, Kullberg J, Cedernaes J, Johansson HE, Larsson A, Johansson L, Ahlström H, Arner P, Dahlman I, Risérus U. 2014. Overfeeding Polyunsaturated and Saturated Fat Causes Distinct Effects on Liver and Visceral Fat Accumulation in Humans. *Diabetes* 63: 2356–2368.
- Sotiras A, Davatzikos C, Paragios N. 2013. Deformable Medical Image Registration: A Survey. *IEEE transactions on medical imaging* 32: 1153–1190.
- Strand R, Malmberg F, Johansson L, Lind L, Sundbom M, Ahlström H, Kullberg J. 2017. A concept for holistic whole body MRI data analysis, Imiomics. *PLOS ONE* 12: e0169966. Publisher: Public Library of Science.
- Summers LKM, Fielding BA, Bradshaw HA, Ilic V, Beysen C, Clark ML, Moore NR, Frayn KN. 2002. Substituting dietary saturated fat with polyunsaturated fat changes abdominal fat distribution and improves insulin sensitivity. *Diabetologia* 45: 369–377.
- Virtanen P, Gommers R, Oliphant TE, Haberland M, Reddy T, Cournapeau D, Burovski E, Peterson P, Weckesser W, Bright J, van der Walt SJ, Brett M, Wilson J, Millman KJ, Mayorov N, Nelson ARJ, Jones E, Kern R, Larson E, Carey CJ, Polat □, Feng Y, Moore EW, VanderPlas J, Laxalde D, Perktold J, Cimrman R, Henriksen I, Quintero EA, Harris CR, Archibald AM, Ribeiro AH, Pedregosa F, van Mulbregt P. 2020. SciPy 1.0: fundamental algorithms for scientific computing in Python. *Nature Methods* 17: 261–272. Number: 3 Publisher: Nature Publishing Group.

## A Appendix

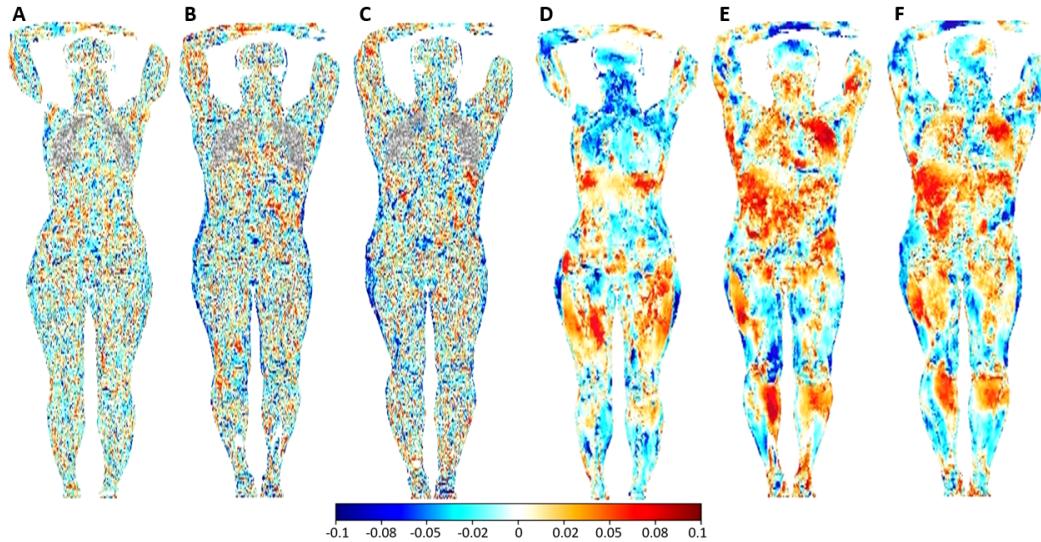


Figure 11: Voxel-wise T-tests between the PUFA and SFA group for the difference in fat content and JD maps. Red color indicates a positive T-statistic, thus a larger mean value in the PUFA group than the SFA group. A blue color indicates a negative T-statistic, thus a smaller mean value in the PUFA group than in the SFA group. The maps have no P-value cutoff. A is the T-test between the difference in fat content of the female PUFA ( $n=6$ ) and SFA ( $n=6$ ) group. B is the T-test between the difference in fat content of the male PUFA ( $n=12$ ) and SFA ( $n=14$ ) group. C is the T-test between the difference in fat content of the PUFA ( $n=18$ ) and SFA ( $n=20$ ) group consisting of both females and males. D is the T-test between the JD maps of the female PUFA ( $n=6$ ) and SFA ( $n=6$ ) group. E is the T-test between the JD maps of the male PUFA ( $n=12$ ) and SFA ( $n=14$ ) group. F is the T-test between the JD maps of the PUFA ( $n=18$ ) and SFA ( $n=20$ ) group consisting of both females and males.